Reconfigurable RF-MEMS Metamaterials Filters

I. Gil[1], **M. Morata**[2], **R. Fernández-García**[1], **X. Rottenberg**[3], **and W. De Raedt**[3]

[1]Department of Electronic Engineering, UPC Barcelona Tech., Colom 1, Terrassa 08222, Spain
[2]Escuela Universitaria Salesiana de Sarriá, Barcelona 08017, Spain
[3]IMEC, Leuven B-3001, Belgium

Abstract— In this work, the design procedure, modelling and implementation of reconfigurable filters based on RF microelectromechanical systems metamaterials is presented. Specifically, tunable stop-band and pass-band frequency responses are obtained by combining RF-MEMS with metamaterials based in complementary split rings resonators. These particles, allow for the design of negative effective permittivity transmission lines, providing forbidden propagation frequency bands. Moreover, CSRRs properly combined with metal vias in transmission lines, generate a simultaneously $\varepsilon < 0$ and $\mu < 0$ effective media which involves an allowed frequency band. These two phenomenons have been used in order to implement stop-band and pass-band filters. Since CSRRs present a LC-tank behaviour and are electrically coupled to the host line, the tunability is achieved by means of the RF-MEMS, which modify the electrical characteristics of the CSRRs and the electric coupling. A full electrical model for the description of the proposed structures is presented. The circuit model take into account the electrical characteristics of the RF-MEMS, CSRRs and transmission lines as well as the involved electromagnetic coupling and are used for accurate prediction of switchable filters response.

1. INTRODUCTION

RF microelectromechanical systems (RF-MEMS) tunable filters have been developed in recent years for military and commercial applications such as multiband communication systems or wide-band transceivers due to their low-power consumption, high quality factor and good linearity [1]. RF-MEMS are typically implemented by means of several lithographic steps which perform RF-MEMS in conventional distributed transmission lines. Alternatively, the combination of metamaterial structures together with transmission lines (i.e., artificial lines consisting of a host line loaded with reactive elements) have been revealed as good candidates in order to improve the performance of conventional distributed passive devices, and specifically those corresponding to microwave filters. In order to deepen the knowledge of designers concerning both RF-MEMS tunable filters and tunable metamaterial transmission lines in PCB, several works have been published including performance and accurate electrical models [2–5]. In this paper, the design procedure, modelling and implementation of reconfigurable filters based on RF-MEMS metamaterials is presented. Specifically, tunable stop-band and pass-band frequency responses are obtained by combining RF-MEMS with complementary split rings resonators (CSRRs) [6]. CSRRs, which are the dual image of split rings resonators (SRRs) [7], allow for the design of negative effective permittivity transmission lines, providing forbidden propagation frequency bands due to the effective behavior of $\varepsilon < 0$ and $\mu > 0$ in a certain frequency band. Moreover, CSRRs properly combined with metal vias in transmission lines, generate a simultaneously $\varepsilon < 0$ and $\mu < 0$ effective media which involves an allowed frequency band. These two phenomenons have been used in order to implement stop-band and pass-band filters.

2. STOP-BAND CSRR/RF-MEMS FILTERS

Figure 1 shows the layout of the proposed stop-band filter prototype. It consists of a $50\,\Omega$ coplanar waveguide structure (CPW) loaded with 4-stages of rectangular shaped CSRRs etched in the metal strip and RF-MEMS bridges over them. The actual RF-MEMS are based on electrostatic parallel-plate varactors which are constituted of a movable electrode mechanically anchored on the substrate and suspended above a second fixed electrode. In fact, RF-MEMS are implemented in the CSRRs by using an electrostatic floating bridge anchored on the substrate in holes of the CPW ground planes. Under DC-bias, the device tends to close, adjusting the capacitance defined by the two plates [8]. Due to the intrinsic instability of this actuation scheme, these devices are used in switch-mode. Only up- and down-states (i.e., small and large capacitance) are functional. A stripped-down RF-MEMS technology using only 3 lithographic steps [9] has been used to define the structures depicted in Fig. 1. First, a $1\,\mu$m thick Al layer is sputter-deposited and patterned

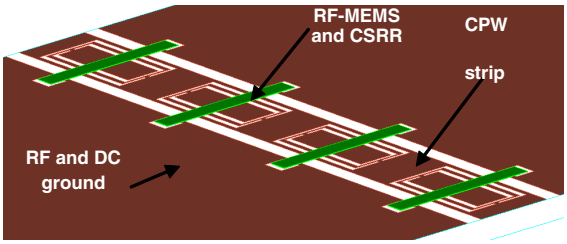

Figure 1: Layout of the 4-stages CSRR/RF-MEMS switchable notch filter.

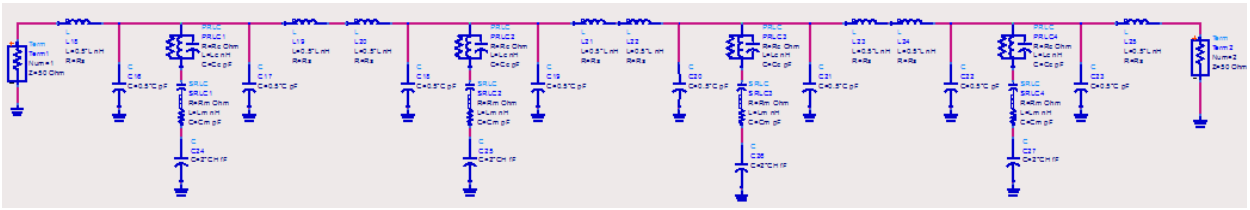

Figure 2: Equivalent lumped circuit model of the filter depicted in Fig. 1.

on a 650 µm thick AF45 glass substrate ($\varepsilon_r = 5.9$) to define mainly the CPW structures. Then, a 3 µm thick sacrificial photoresist layer is spun and patterned to define the anchoring regions of the MEMS devices before a second Al layer is deposited and patterned in the same way as the first one. Therefore, the MEMS beams are defined. Finally, the sacrificial photoresist is ashed to release the devices. Due to the variable capacitance of the RF-MEMS and its coupling to the host transmission line, the effective capacitance of the CSRRs can be modified, and hence, their intrinsic resonance frequency. A full electrical model for the description of the proposed structures is presented in Fig. 2. The circuit models take into account the electrical characteristics of the RF-MEMS, CSRRs and transmission lines as well as the involved electromagnetic coupling and are used for accurate prediction of switchable filters response. The lienRF-MEMS bridges are modelled by means of a lumped RLC series circuit, with a variable capacitance, C_M, (having an up-state and a down-state value), L_M is the bridge inductance and the resistor R_M involves the microelectromechanical system losses. The anchoring capacitance of the CPW holes is modelled by C_H. The CPW line is described by means of the per-section inductance, L, and capacitance, C. The etched CSRRs are modelled by means of a parallel RLC tank, L_C and C_C being the reactive elements which constitute the intrinsic resonance frequency of the resonators and RC takes into account the eventual losses associated with the resonator. CSRRs are directly connected to the host line and electrically coupled to the capacitance of the RF-MEMS. Therefore, the intrinsic resonance frequency of the subwavelength resonators, f_o, (1) is directly affected by the RF-MEMS actuation. As a result of this behaviour, a reconfigurable stop-band frequency response is achieved, which corresponds to the condition which nulls the impedance of the shunt equivalent branch, Z_S, constituted by the impedances of the RF-MEMS, CSRRs, anchoring capacitance and host line capacitance, according to (2):

$$f_o = \frac{1}{2\pi\sqrt{L_C C_C}}, \tag{1}$$

$$Z_S = 0 \Rightarrow \frac{j\omega L_C R_C}{R_C - \omega^2 R_C L_C C_C + j\omega L_C} + \frac{R_C - \omega^2 L_M \left[2C_H C_M/(2C_H + C_M)\right] + j\omega R_M \left[2C_H C_M/(2C_H + C_M)\right]}{j\omega \left[2C_H C_M/(2C_H + C_M)\right]} = 0. \tag{2}$$

The presented model has been electrically simulated by using the commercial *Agilent ADS* and validated by comparison with electromagnetic simulation (i.e., layout simulation with *Agilent Momentum*) and experimental test (a HP8510C vector network analyzer and G-S-G test probes having coaxial connectors type 2.4 mm, have been used). Fig. 3 shows the comparison between the measured data, electromagnetic simulations and the proposed lumped model insertion losses (S_{21}). Both, the up and down state have been electromagnetically simulated by considering a parallel

plate to the host line. Layout simulation has been carried out by considering planar plate heights of 0.5 µm (down-state) and 2 µm (up-state), respectively and no losses have been assumed. As expected, the structure exhibits stop-band behaviour with reconfigurable capability. The simulated frequency range corresponds to 39–48.8 GHz (Q-band), which implies to a switching range of roughly 20%. As can be seen, good matching level between the involved notch frequencies concerning the model prediction is achieved. However, the band edges, related with the quality factor, as well as the rejection level are not correctly reproduced due to the intrinsic lossless simplicity. Electromagnetic simulated rejection levels are $IL < -50$ dB whereas model predicts higher notch rejection levels. Regarding experimental results, the RF-MEMS have been subjected to actuation voltage, caused by an external polarization, from 17 V (down-state) to 0 V (up-state). A significant agreement with respect to the full equivalent circuit model including losses is achieved, not only concerning the tuning range (experimental values are 39–48.1 GHz, whereas model correspond to 38.9–47.5 GHz), but also in terms of rejection level (experimental $ILD = -43$ dB; $ILU = -40.9$ dB and model $ILD = -50.4$ dB; $ILU = -40.2$ dB) and quality factor (experimental $QD = 30.9$; QU is not determined due to the limitation up to 50 GHz in the setup, and model $QD = 29.7$; $QU = 29.5$).

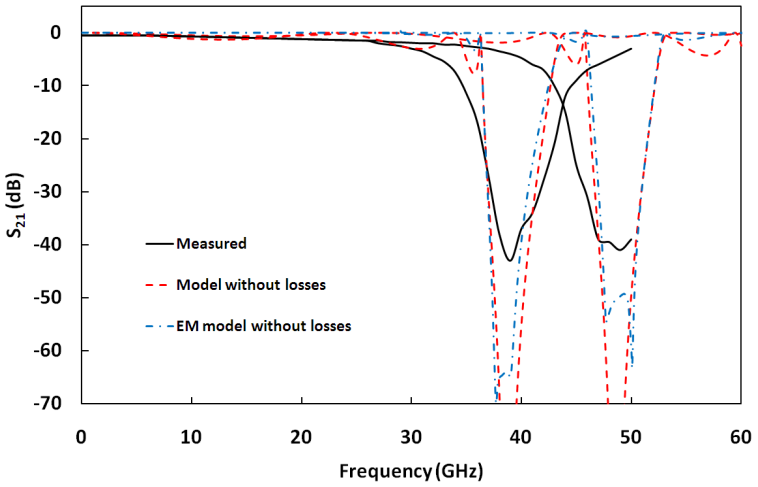

Figure 3: Frequency response transmission (insertion losses) corresponding to the up and down-state of the stop-band CSRR/RF-MEMS filter. Experimental data, electromagnetic simulations and electrical model are shown.

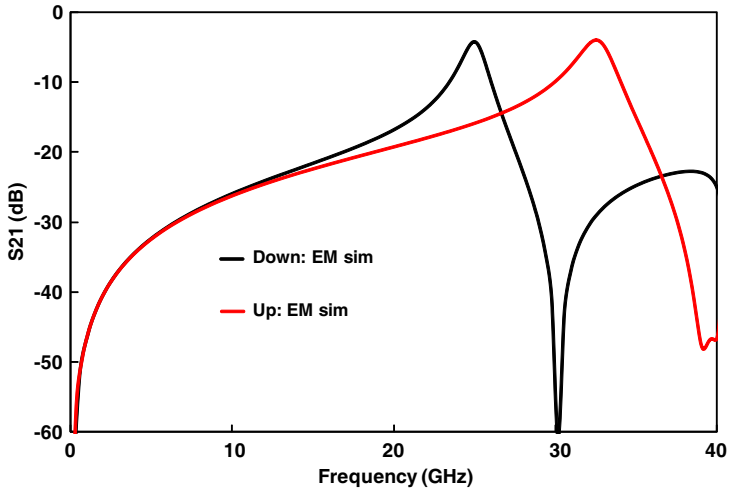

Figure 4: Frequency response transmission (insertion losses) corresponding to the up and down-state of the pass-band CSRR/RF-MEMS filter. Electromagnetic simulations are shown.

3. PASS-BAND CSRR/RF-MEMS FILTERS

In order to obtain a band-pass filter response, a similar unit cell topology than in Fig. 1 can be reused by adding two metal wires (per stage) connecting the central CPW strip and the ground planes in order to achieve an effective band pass frequency response. In fact, due to the equivalent $\mu < 0$ behaviour of the metal wires combined with the $\varepsilon < 0$ of the CSRRs, an allowed band in a certain frequency band is obtained. Fig. 4 shows the electromagnetic simulation of a 50 Ω CPW structure loaded with 1-stages of rectangular shaped CSRR etched in the metal strip and RF-MEMS bridges over them including the extra metal wires connecting host line and ground. As expected, a pass-band CSRR/RF-MEMS filter is obtained. The frequency range is different with regard to Fig. 3, since other subwavelength resonators' dimensions have been considered. This structure is now pending of fabrication and work is in progress in order to evaluate its experimental performance.

4. CONCLUSIONS

Several tunable stop-band and pass-band filter, based on the combination of complementary split ring resonators and RF-MEMS switchable capacitors have been presented and characterized as proof-of concept. The measured frequency responses of the device for different actuation voltages are good and significant tuning range has been achieved for stop-band responses. Results are promising for pass-band structures and work is currently in progress.

ACKNOWLEDGMENT

This work has been supported by the Spain-MICINN under Project TEC2009-09994 and AGAUR 2009 SGR 1425.

REFERENCES

1. Rebeiz, G. M., *RF MEMS: Theory, Design and Technology*, John Wiley & Sons, 2003.
2. Entesari, K. and G. M. Rebeiz, "A 12–18 GHz three-pole RF MEMS tunable filter," *IEEE Transactions on Microwave Theory and Techniques*, Vol. 53, 2566–2571, August 2005.
3. Entesari, K., K. Obeidat, A. R. Brown, and G. M. Rebeiz, "A 25–75 MHz RF MEMS tunable filters," *IEEE Transactions on Microwave Theory and Techniques*, Vol. 55, 2399–2405, November 2007.
4. Bonache, J., I. Gil, J. García-García, and F. Martín, "Novel microstrip band pass filters based on complementary split rings resonators," *IEEE Transactions on Microwave Theory and Techniques*, Vol. 54, 265–271, January 2006.
5. García-García, J., F. Martín, E. Amat, F. Falcone, J. Bonache, I. Gil, T. Lopetegi, M. A. G. Laso, A. Marcotegui, M. Sorolla, and R. Marqués, "Microwave filters with improved stop band based on sub-wavelength resonators," *IEEE Transactions on Microwave Theory and Techniques*, Vol. 53, 1997–2006, June 2005.
6. Falcone, F., T. Lopetegi, J. D. Baena, R. Marqués, F. Martín, and M. Sorolla, "Effective negative-ε stopband microstrip lines based on complementary split ring resonators," *IEEE Microwave Wireless Compon. Lett.*, Vol. 14, 280–282, June 2004.
7. Pendry, J. B., A. J. Holden, D. J. Robbins, and W. J. Stewart, "Magnetism from conductors and enhanced nonlinear phenomena," *IEEE Transactions on Microwave Theory and Techniques*, Vol. 47, 2075–2084, November 1999.
8. Varadian, V. K., K. J. Vinoy, and K. A. Jose, *RF MEMS and Their Applications*, John Wiley & Sons, 2003.
9. Rottenberg, X., S. Brebels, P. Ekkels, P. Czarnecki, P. Nolmans, R. P. Mertens, B. Nauwelaers, R. Puers, I. De Wolf, W. De Raedt, and H. A. C. Tilmans, "Electrostatic fringing-field actuator (EFFA): Application towards a low-complexity thin-film RF-MEMS technology," *J. Micromech. Microeng.*, Vol. 17, S204–S210, 2007.